Available online at www.sciencedirect.com
SCIENCE DIRECT®
Physics Letters A 347 (2005) 121–132
PHYSICS LETTERS A
www.elsevier.com/locate/pla

Einstein's impact on optics at the frontier

Donald Umstadter

Physics and Astronomy Department, University of Nebraska, Lincoln, NE 68588-0111, USA

Received 3 June 2005; received in revised form 27 August 2005; accepted 6 September 2005

Available online 21 September 2005

Communicated by F. Porcelli

Abstract

The seminal contributions made by Einstein a century ago have enabled a new frontier area of science, called high-field science. This research involves the physics of the interactions of matter with electromagnetic fields at its highest levels ever achieved in the laboratory. Besides being of fundamental importance to physics research, the discoveries being made in this area are also leading to a new generation of compact and ultrashort-duration particle accelerators and X-ray light sources, with applications ranging from nuclear fusion to cancer therapy.

1. Orientation and background

1.1. Introduction

In 1905, a century ago, the year referred to by some as Einstein's annus mirabilis (miracle year), the highest peak power of light was more than twenty orders-of-magnitude lower than it is today (see Fig. 1). And yet, in his series of brilliant papers from that year, Einstein established the fundamental physical principles that today govern the interactions of light with matter at this "unimaginably" higher power level. The physics involved in today's high-power-laser research involves the nonlinear optics of the highest electromagnetic field strengths ever achieved in the laboratory. This research is leading to a new generation of compact and ultrashort-duration particle accelerators and X-ray light sources, with applications ranging from nuclear fusion to cancer therapy.

Research in this area is one of the best examples illustrating how Einstein's was a century ahead of his time. For example, without his paper on the quantum nature of light, the laser itself, which is critical for this research, would never have been possible. Without his paper on special relativity, the nonlinear optical effects observed at these laser intensities would be incomprehensible. Last, Einstein's paper on Brownian motion was the first study of atomic and molecular dynamics, which is one of the primary applications of today's research with the ultrashort pulse duration light sources.

In this Letter, we present a summary of the current status of research with ultra-high intensity and ultra-

E-mail address: dpu@unlserve.unl.edu (D. Umstadter).

0375-9601/$ – see front matter
doi:10.1016/j.physleta.2005.09.005

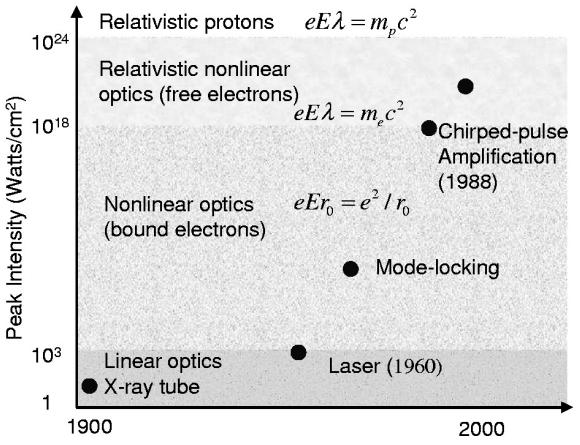

Fig. 1. History of light sources over the last century. Each advance in laser power enables a new regime of optics. Reproduced from [33].

short duration laser light, and show how it connects with Einstein's visionary work of a century earlier.

1.2. Relativistic optics and high field science

In 1905, the most powerful laboratory light source was the X-ray tube, which produced approximately 1 kW of peak power. The electromagnetic field strength produced by such a source was quite minuscule when compared to the field that binds the electron to the nucleus. Thomson had just discovered at this time that light scattered from an electron was emitted at the same frequency as the light that was incident, and that the electron would follow the electric field of the light wave. In 1960, nearly half a century later, the laser was invented, which as based upon Einstein's quantum theory of light. With the ensuing dramatic increase in power, light could be focused to sufficient intensity to cause nonlinear optical effects in atomic media. In conventional nonlinear optics, where the electric field of a light wave E is much smaller than an atomic field, $E_{\text{at}} = 3 \times 10^9$ V/cm, various nonlinear phenomena, such as self-focusing, harmonic generation and Raman scattering, arise due to the anharmonic motion of electrons in the combined fields of atom and laser. Approximate analytical solutions can be obtained by means of perturbation expansion methods, using E/E_{at} as the expansion parameter. At higher light fields, when E approaches E_{at}, this method breaks down and the medium becomes photo-ionized, creating a plasma, as illustrated by Fig. 2. Further increases in light intensity enabled nonlinear optical effects of even these free plasma electrons (see Fig. 1). The nonlinearity arises in this case because the electrons oscillate at relativistic velocities in laser fields that exceed 10^{11} V/cm, resulting in relativistic mass changes that exceed the electron rest mass and the light's magnetic field becoming important. The work done by the electromagnetic field (E) on an electron ($eE\lambda$) over the distance of a laser wavelength (λ) then approaches the electron rest mass energy ($m_e c^2$), where e is the elementary charge of an electron, m_e is the electron rest mass and c is the speed of light. Effects analogous to those studied with conventional nonlinear optics—self-focusing, self-modulation, harmonic generation, and so on—are all found, but based on this entirely different physical mechanism. Thus, a new field of nonlinear optics, that of relativistic electrons, has been launched, as illustrated by Fig. 2.

One outcome of accessing this new optical regime is the generation of ultra-short duration frequency-shifted light in a spectral region where there are no other compact sources. Another is the acceleration of other types of particles, such as positrons, ions and neutrons. These novel radiation sources have properties (femtosecond duration, micron source size, MeV energy) that make them suitable for numerous applications in imaging and spectroscopy in basic research, as well as medical diagnostics, cancer therapy, energy production and space propulsion. Rapid advancement is underway and new research tools, subfields and commercial products are on the horizon: e.g., compact and ultrashort pulse duration laser-based electron accelerators and X-ray sources.

Another physical regime will be encountered at even higher intensities ($I\lambda^2 \simeq 10^{24}$ W/cm^2), when even protons will quiver relativistically: i.e., the work done on an proton over the distance of a laser wavelength approaches the rest mass energy. This might be called the nuclear regime of laser–plasma interactions, because of the fusion and fission reactions and the generation of pions, muons and neutrinos that should occur as nuclei collide in such energetic plasmas.

For more detailed descriptions of recent progress in experiments and theory, several review papers have been published on related topics: (1) relativistic nonlinear optics [25,31,33–35], (2) high-intensity laser development [26], (3) laser accelerators [9], (4) intense laser–plasma interactions [13,15,18,23,24,33],

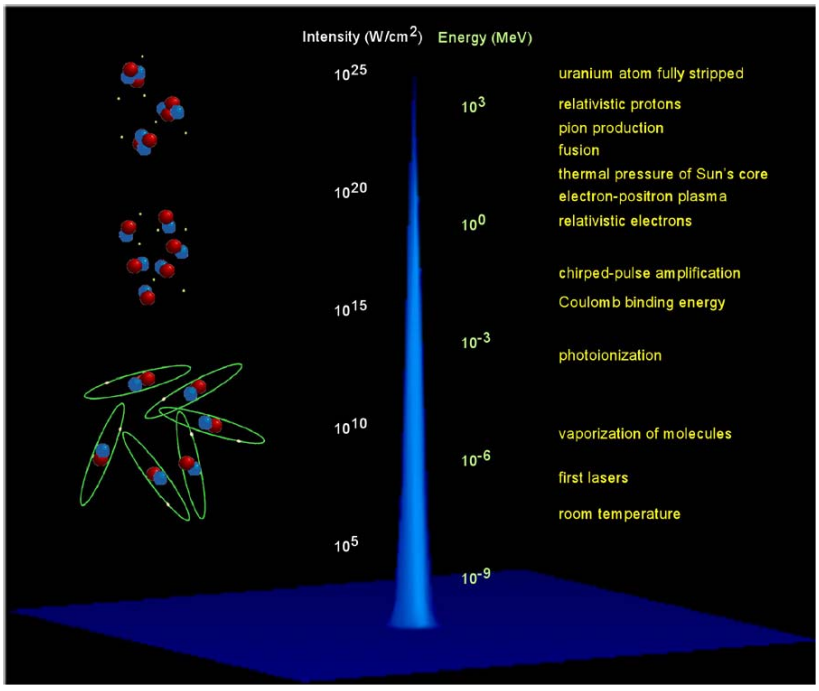

Fig. 2. The various regimes of laser–matter interactions, represented by the ideal laser pulse. As the intensity of laser light increases, so does the energy of electrons accelerated in the light field and the regime of conventional nonlinear optics with electrons bound to atoms is replaced by the regime of relativistic nonlinear optics with free electrons in relativistic plasmas. At the highest intensities, even protons become relativistic, giving rise to what might be called the regime of nuclear optics, in which various nuclear processes, such as fusion, can take place. Reproduced from [33].

(5) relativistic scattering [8,14,17], and (6) light ion acceleration [22].

2. Single-particle motion in high electromagnetic fields

An electron that is in the field of an electromagnetic wave propagating in the $+z$ direction has an orbit that is governed by the Lorentz equation,

$$m\frac{d\mathbf{v}}{dt} = -e\left(\mathbf{E} + \frac{\mathbf{v}}{c} \times \mathbf{B}\right), \tag{1}$$

where $\mathbf{v}$ is the electron velocity, and $\mathbf{E}$ and $\mathbf{B}$ are the light's electric and magnetic fields.

A zeroth order solution to Eq. (1) is found by setting $\mathbf{v}/c \ll 1$, which allows the term $(\mathbf{v}/c) \times \mathbf{B}$ to be neglected and γ is set to unity. Integrating Eq. (1) in this limit once over time (t) yields the following equations for the velocity, where "LP" signifies "linear polarization", and "CP" signifies "circular polarization",

$$\mathbf{v} = \mathrm{Re}\left\{\frac{e\mathbf{E}}{im\omega}\right\} = a_0 c \begin{cases} \hat{e}_x \cos\psi, & \text{LP}, \\ (\hat{e}_x \cos\psi \mp \hat{e}_y \sin\psi), & \text{CP}. \end{cases} \tag{2}$$

An electron in low-intensity light oscillates with this velocity in a straight line along the polarization vector ($\hat{e}_y$), which when normalized to c, is the normalized vector potential $a_0 \equiv eE_0/m_e\omega c$. Integrating again yields for the transverse displacement

$$\mathbf{x} = \mathrm{Re}\left\{\frac{e\mathbf{E}}{m\omega^2}\right\} = a_0 c \begin{cases} \hat{e}_x \sin\psi, & \text{LP}, \\ (-\hat{e}_x \sin\psi \mp \hat{e}_y \cos\psi), & \text{CP}. \end{cases} \tag{3}$$

Thus, for the $a_0 \sim 1$, the electron excursion during its oscillation is approximately λ.

A first order approximation for the electron motion can be found by substituting the zeroth order velocity Eq. (2) into the $\mathbf{v}/c \times \mathbf{B}$ term of (1). The latter then

becomes proportional to

$$\mathbf{E}\times\mathbf{B}\propto\frac{a_0^2}{2}\bigl[1+\cos(2\omega_0)\bigr]\hat{e}_z. \tag{4}$$

In the frame in which the electron is on the average at rest, the relativistic motion of an electron is thus described by a figure eight, oscillating twice in the $\hat{e}_z$ or $\hat{k}$ direction for every once in the polarization direction ($\hat{e}_x$); i.e., a figure of eight motion. This originates from the fact that $\mathbf{v}\times\mathbf{B}\propto\mathbf{E}\times\mathbf{B}\propto\mathbf{E}^2\hat{k}$, which is a product of two functions that vary sinusoidally at frequency ω and thus varies itself at frequency 2ω. In the lab frame, this transverse motion is superimposed upon a steady drift in the ($\hat{e}_z$) direction, originating from the DC term in Eq. (4). The next order approximation would include the mass shift $m=\gamma m_e$. As the field strength increases ($a_0^2\gg 1$), the longitudinal motion ($\propto a_0^2$) begins to dominate the transverse motion ($\propto a_0$).

In the regime $a_0\lesssim 1$, electrons radiate photons at harmonics of a modified laser frequency ω_0, with each harmonic order having its own unique angular distribution. The radiation at the fundamental is the usual donut pattern, with a maximum in the direction perpendicular, and a minimum along, the polarization vector ($\hat{e}_x$). The second harmonic has two emission lobes with maxima pointing at angles between $\hat{e}_z$ and $\hat{e}_x$. A additional lobe is added for each additional harmonic order. This is referred to as nonlinear or relativistic Thomson scattering. The unique angular distributions of the second and third harmonics emitted from nonlinear relativistic Thomson scattering were observed experimentally [5]. As will be shown in detail in Section 4, the situation is more complex for $a_0\gtrsim 1$, and the scattered light is no longer simply harmonic.

The Lorentz equation was modified by Einstein's special theory of relativity to correct for the change in the electron mass:

$$\frac{d\mathbf{p}}{dt}=m_0\frac{\partial}{\partial t}(\gamma\mathbf{v})=q\left[\mathbf{E}+\frac{1}{c}\mathbf{v}\times\mathbf{B}\right], \tag{5}$$

where $\mathbf{p}$ is the particle momentum, m_0 is the rest mass, $\gamma=(1-\mathbf{v}^2/c^2)^{-1/2}$ is the Lorentz factor, and q is the particle's charge. Using this equation, it can be shown that the angle θ at which an electron scatters is related to the transverse and longitudinal momenta or the kinetic energy by:

$$\tan^2\theta=\left(\frac{p_\perp}{p_z}\right)^2=\frac{2mE_{\mathrm{kin}}}{(E_{\mathrm{kin}}/c)^2}=\frac{2}{\gamma-1}. \tag{6}$$

In fact, this relation can be readily extended to the case of an electron with a nonzero initial kinetic energy, $E_{\mathrm{kin}}(t=0)=(\gamma_0-1)m_0c^2$ yielding

$$\tan^2\theta=\frac{2(\gamma/\gamma_0-1)/(1+\beta_0)}{[\gamma-\gamma_0(1-\beta_0)]^2}, \tag{7}$$

where β_0 is the initial electron speed normalized to the speed of light. The angle of electrons produced by photo-ionization with intense lasers has been shown experimentally to obey the conservation of canonical momentum, as demonstrated in experiments that studied the angular distribution of relativistic electrons emitted from barrier-suppression ionization of atoms in intense laser fields, discussed in detail by Meyerhofer et al. in [34]. As the laser waist and pulse duration shrink and the intensity rises, this plane wave model eventually fails. This has demonstrated, for example, in simulations by Quesnel and Mora [27].

3. Direct laser acceleration of electrons in vacuum

The Lawson–Woodward theorem states that in linear systems under certain conditions an electron can gain no net energy from a laser pulse. As the strength of the laser field increases, however, the Lorentz force introduces a nonlinearity to the problem, and energy can be transferred directly from the laser to the electron. The amount of energy is still limited by relativistic considerations, though. Since any charged mass necessarily travels at less than the speed of light, c, the laser light will overtake the particle. Thus, an electron cannot lock into a phase that constantly generates a positive acceleration. Instead, the electron alternates in a cycle of positive and negative acceleration yielding the figure-eight motion of an electron in a plane wave laser. When the laser is focused, the phase fronts become curved. Each point on these fronts travels at c along the propagation direction $\mathbf{k}$, but they do not cross a given plane normal to $\mathbf{k}$ at the same time. Therefore, an electron possessing the correct phase and velocity can observe a local phase velocity somewhat less than c by riding this curvature and can be

accelerated to high energies by surfing these phase fronts without violating special relativity.

The gradients of focused transverse laser fields can be used to accelerate and deflect electrons in vacuum for all angles of incidence through the ponderomotive force. The longitudinal field component of a tightly focused ultra-intense light beam can also play an important role. It can act to deflect a beam of energetic electrons, as was recently demonstrated experimentally. 100-keV energy electrons were deflected by a laser with $a_0 = 1$, corresponding to a 1-μm laser intensity of 3.46×10^{18} W/cm^2 [1]. It has been shown theoretically that for $a_0 = 10$, corresponding to a 1-μm laser intensity of 3.46×10^{21} W/cm^2, relativistic electrons, with an energy as high as 10 MeV, can be deflected.

In this experiment, the authors focused a terawatt-power laser onto a beam of electrons (which had been accelerated by a plasma wave, driven by another synchronized laser pulse). The laser was pointed in a direction perpendicular to the direction in which the electrons were propagating. When a laser beam is unfocused, it is true that it can be approximated as a plane wave, and the electric and magnetic fields are indeed primarily pointing in a direction that is perpendicular to the direction of propagation of the light wave. But, when laser light is tightly focused, the phase fronts become curved, and a significant fraction of the fields will then point towards the direction of propagation of the light wave. Through the familiar Lorentz force, these fields acted to accelerate the electrons in the same direction in which the fields were pointing. A camera placed downstream from the electron beam was used to measure the angle the electrons had been deflected by the light beam. This result represents the first experimental verification of several recent theories on laser acceleration of electrons in free space. Previous experimental results yielded results that were inconsistent with theory. But, not only is this discovery important from the point of view of fundamental physics, it also has several interesting and novel applications.

Using this technique, a single bunch of electrons with femtosecond duration was sliced out of the picosecond-long electron beam. This optical conditioning of energetic electron beams can be used to probe ultrafast physical and chemical dynamics on ultrashort time scales. Either the electrons can be used directly for this purpose, such as in time-resolved electron diffraction, or ultrashort duration X-rays (that can be produced by Thomson scattering) can be used. In their experiment, the authors also demonstrated that their technique could be used to directly measure ultrashort electron bunch durations.

4. Radiation from relativistic electrons

The harmonic generation discussed above in the nonrelativistic regime have studied theoretically in the relativistic regime by [17]; detailed discussions can also be found in Leemans et al., in Meyerhofer et al., and in [34].

To summarize the results, it is found that due to the rapid acceleration of electrons in the direction of the light wave and decrease of the oscillation frequency in the deeply relativistic regime, the photon energy from relativistic nonlinear scattering scales only linearly with laser field strength, $\sim a_0$. However, the relativistic motion of the electron results in a reduction in the angle of the scattered light, such that the harmonics are generated in a low-divergence-angle forward-propagating beam. There is also a relativistic Doppler shift ($\sim \gamma^2$). For instance, this mechanism will be used in high-energy physics experiments to cleanly make constituent particles in the gamma–gamma ($\gamma\gamma$) collider, in which gamma rays with energy 200 GeV will be generated by Compton scattering 1 eV photons from 250-GeV energy conventionally accelerated electron beams ($\gamma = 5 \times 10^{11}$).

Using a much smaller, laser-based accelerator (discussed in Section 7), a 1 eV photon can be upshifted by this Doppler shift to an energy of 50 keV, corresponding to sub-atomic spatial resolution and of interest in medical diagnostics, by an electron beam with only $\gamma = 200$ (100 MeV). In this case, the maximum efficiency is obtained for laser fields a_0 of order unity. When compared with conventional light sources based on cm-wavelength magnetostatic wigglers, the electromagnetic wigglers of such an all-optical-laser-based EUV sources have ten-thousand times shorter wavelength (micron-scale). Thus, the total length of the wiggler region is correspondingly smaller (only mm in length). Another consequence of this is that the frequency upshift required to reach a given output wavelength is also ten-thousand times smaller. Also,

given that the required electron energy scales as the square root of the upshift, the required electron energy can be one-hundred-times lower (10–100 MeV). It follows from this, and the fact that the field gradients of these accelerators can be ten-thousand-times higher (1 GeV/cm) than convention RF-based accelerators, that the size of the accelerating region can in principle be a million times smaller (only mm in length). Besides its small size, this EUV source can produce femtosecond duration pulse and be synchronized with a relatively low jitter with another femtosecond light pulse having a different wavelength (by virtue of the possibility of deriving the two pulses from the same laser pulse); this is advantageous for the study of ultrafast pump-and-probe photo-initiated processes. The exceptionally low transverse emittance of laser-accelerated electron beams may even make it possible to generate coherent XUV radiation by means of the self-amplified spontaneous emission (SASE) free-electron lasing (FEL) mechanism.

5. Propagation in a dielectric medium

To understand the propagation of high-intensity light in plasma, we need to understand how the dielectric properties of a plasma medium are affected by the relativistic electron mass change (see e.g. Esarey in [34]). A wave equation is found from Maxwell's equations, assuming a uniform plasma, and Eq. (2) for the velocity:

$$\left(-\frac{\partial^2}{\partial t^2} + c^2\nabla^2 - \omega_p^2\right)\mathbf{E} = 0, \tag{8}$$

where

$$\omega_p = \left(4\pi n_j q_j^2/m_j\right)^{1/2}$$

is the plasma frequency. Assuming again plane waves and Fourier analyzing, yields the well-known dispersion relation for electromagnetic waves in plasma,

$$\omega^2 = \omega_p^2 + c^2k^2. \tag{9}$$

The index of refraction can be written fully relativistically as

$$\eta^2 = \frac{c^2k^2}{\omega^2} = \frac{c^2}{v_\phi^2} = 1 - \frac{\omega_p^2}{\omega^2}, \tag{10}$$

where v_ϕ is the phase velocity of the light wave. Assuming infinitely massive ions, the plasma frequency can be written as

$$\omega_p = \frac{\omega_{p0}}{\gamma^{1/2}} = \left(\frac{4\pi n_e e^2}{\gamma m_0}\right)^{1/2}, \tag{11}$$

where ω_{p0} is the plasma frequency in a quiescent plasma, e is the electron charge, m_0 is the electron rest mass, and n_e is the plasma electron density. A change in mass changes the plasma frequency, which in turn modifies the index of refraction and the velocity of the light wave. For an underdense plasma, $\omega_p^2 \ll \omega_0^2$, the plasma refractive index can be Taylor expanded, and written as

$$\eta = \sqrt{1 - \frac{\omega_p^2}{\omega_0^2}} = 1 - \frac{\omega_p^2}{2\omega_0^2} \simeq 1 - \frac{n_e}{2n_c\gamma}, \tag{12}$$

where n_c is the critical electron density and is equal to $\omega_0^2 m_e/4\pi e^2$. When $a \leqslant 1$, the plasma refractive index can be further simplified by expanding about a_0, which results in

$$\eta = 1 - \left(1 - \frac{\langle a_0^2\rangle}{2}\right)\frac{n_e}{2n_c} = n_1 + n_2 I, \tag{13}$$

where $n_1 = 1 - n_e/2n_c$ and $n_2 = (8.5 \times 10^{-10}\lambda\ [\mu\text{m}])^2 n_e/8n_c$. The light's phase velocity then depends on the laser intensity. This can be seen clearly if we expand the phase velocity for small field strength ($a_0 \leqslant 1$),

$$v_\phi = \frac{c}{\eta} \sim c\left[1 + \frac{\omega_{p0}^2}{2\omega^2}\left(1 - \frac{\langle a_0^2\rangle}{2}\right)\right], \tag{14}$$

where $\langle a_0^2\rangle$ denotes the time averaged value of the normalized vector potential. An on-axis minimum of the phase velocity [i.e., $v_\phi(r) > v_\phi(0)$] can be created by a laser beam with an intensity profile peaked on axis, such as with a Gaussian beam, causing the wavefronts to curve inward and the laser beam to focus, as shown in Fig. 3. When this focusing effect just balances the defocusing caused by diffraction, the laser pulse can propagate over a longer distance than it could in vacuum, while maintaining a small cross section. This mechanism is referred to as relativistic self-guiding.

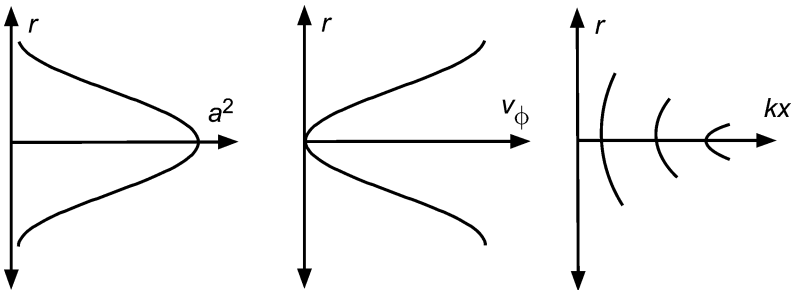

Fig. 3. Relativistic self-focusing occurs when an on-axis peak in light intensity (left) produces an on-axis dip in the phase velocity (middle), which acts like a positive lens to cause the phase fronts to curve inward (right). Reproduced from [33].

6. Relativistic self-focusing

Relativistic self-focusing occurs when a radial change in the index of refraction, which is induced by a Gaussian radial intensity profile, just balances defocusing due to diffraction [21]. Here, again, it is the relativistic mass change that gives rise to the change in the index of refraction. The threshold, critical, power for relativistic self-focusing is given by

$$P_{\text{crit}} \simeq 17.4 \cdot (\omega/\omega_p)^2 \text{ GW}. \tag{15}$$

This corresponds to 1 TW for 1-μm light focused into a gas with electron density of 10^{19} cm^{-3}. Note that this is a power threshold, not an intensity threshold, because the tighter the focusing, the greater the diffraction. Numerous recent experiments have confirmed this focusing mechanism when $P > P_{\text{crit}}$ (see, e.g., [10]).

Any spatial variation of the laser intensity will act to push an electron to regions of lower intensity through the so-called ponderomotive force,

$$\mathbf{F} = \nabla\gamma = \nabla\sqrt{1+a_0^2} = (2\gamma)^{-1}\nabla a_0^2, \tag{16}$$

$$\mathbf{F}_{\text{pond}} = -\frac{m_0c^2}{8\pi}\frac{\nabla a_0^2}{\sqrt{1+\frac{a_0^2}{2}}} \times\left[\left(\frac{2}{a_0^2}+1\right)E(2\pi,\kappa) - \frac{2}{a_0^2}F(2\pi,\kappa)\right], \tag{17}$$

where

$$\kappa = \frac{a_0^2/2}{1+a_0^2/2},$$

and F and E are the elliptic integrals of the first and second kind, respectively. In the low intensity limit, i.e., when $a_0^2 \ll 1$,

$$\mathbf{F}_{\text{pond}} = -\frac{m_0c^2}{4}\nabla a_0^2. \tag{18}$$

That is, the laser ponderomotive force is roughly proportional to the gradient of laser intensity.

A Gaussian-shaped laser's ponderomotive force will tend to expel electrons radially from the region of the axis, so-called "electron cavitation". If the ponderomotive force is high enough for long enough, the charge displacement due to expelled electrons (in either the lateral or longitudinal direction) will eventually cause the ions to move as well through the Coulomb electrostatic force, forming a density channel. Because $n_e(0) < n_e(r)$, and thus $v_\phi(0) < v_\phi(r)$, this enhances the previously-discussed relativistic self-guiding and can itself guide a laser pulse.

For plasmas created by photo-ionization of a gas by a Gaussian laser pulse, the density will be higher on the axis than off the axis. If we instead expand the phase velocity in terms of changes in density,

$$\frac{v_\phi}{c} \sim 1 + \frac{\omega_{p0}^2}{\omega^2}\frac{\Delta n_e}{n_e}. \tag{19}$$

The phase velocity will thus be higher on axis, which will tend to defocus the light and increase the self-guiding threshold. In order to avoid this, gases with low atomic number and thus fewer available electrons, such as H_2, are commonly used as targets.

7. Raman scattering, plasma wave excitation and electron acceleration

The local phase velocity, described in Eqs. (14) and (19), can also vary longitudinally if the intensity

and/or electron density does. Local variation in the index of refraction can "accelerate" photons, i.e., shift their frequency, resulting in photon bunching, which in turn bunches the electron density through the ponderomotive force (F), and so on (e.g., see Mori in [34]). When the laser pulse duration is longer than an electron plasma period, $\tau \gg \tau_p = 2\pi/\omega_p$, this photon and electron bunching grows exponentially, leading to the stimulated Raman scattering instability. Energy and momentum must be conserved when the electromagnetic wave $(\omega_0, \mathbf{k}_0)$ decays into a plasma wave $(\omega_p, \mathbf{k}_p)$ and another light wave $(\omega_0 - \omega_p, \mathbf{k}_0 - \mathbf{k}_p)$.

From an equivalent viewpoint, the process begins with a small density perturbation, Δn_e, which, when coupled with the quiver motion, Eq. (2), drives a current $J = \Delta n_e e v_e$. This current then becomes the source term for the wave equation, driving the scattered light wave. The ponderomotive force due to the beating of the incident and scattered light wave enhances the density perturbation, creating a plasma wave and the process begins anew. In three dimensions, a plasma wave can be driven when transverse self-focusing and stimulated Raman scattering occur together, a process called the self-modulated wakefield instability.

Two conditions must be satisfied for self-modulation to occur in the plasma. First, the laser pulse must be long compared to the plasma wave, $L \gg \lambda_p$. This allows the Raman instability time to grow, and it allows for feedback from the plasma to the laser pulse to occur. Second, the laser must be intense enough for relativistic self-focusing to occur, $P > P_c$, so that the laser can be locally modified by the plasma. Under these conditions, the laser can form a large plasma wave useful for accelerating electrons.

As the long laser pulse enters the plasma, it will begin to drive a small plasma wave due to either forward Raman scattering or the laser wakefield effect from the front of the laser pulse. This small plasma wave will have regions of higher and lower density with both longitudinal and radial dependence. That is, the plasma wave will be three-dimensional in nature with a modulation along the propagation direction of the laser and a decay in the radial direction to the ambient density. The importance of this lies with how it affects the index of refraction in the plasma. In the regions of the plasma wave where the plasma density is lower, the radial change in the index of refraction is negative, $\partial n(r)/\partial r < 0$. This means that this part of the plasma acts like a positive lens and focuses the laser. Whereas regions of the plasma wave where the density is higher, $\partial n(r)/\partial r > 0$, the opposite occurs and the laser defocuses. This has the effect of breaking up the laser pulse into a series of shorter pulses of length $\lambda_p/2$ which will be separated by the plasma period. The instability occurs because of how the plasma responds to this. Where the laser is more tightly focused, the ponderomotive force will be greater and will tend to expel more electrons. This decreases the density in these regions even further, resulting in more focusing of the laser. This feedback rapidly grows, hence the instability.

The Raman instability is due to the positive feedback between the interaction of the plasma density disturbance and the Raman generation. As the disturbance of the electron density seeds the Raman, the Raman, then, will beat with fundamental laser pulse and form an interfere pattern. The ponderomotive force generated from the interference patter will further enhance the electron density fluctuation. Due to this feedback loop, an instability is possible.

The phase velocity of the plasma wave in the case of forward scattering is equal to the group velocity of the beat wave, which for low-density plasma is close to the speed of light, as can be seen from the relation

$$v_\phi = \omega_p/\mathbf{k}_p = \Delta\omega/\Delta k = v_g = c\eta \sim c,$$

where Eq. (10) and $\omega_p^2 \ll \omega^2$ were used to show that η is close to unity. Such relativistic plasma waves can also be driven by short pulses ($\tau \sim \tau_p$). In this case the process is referred to as laser-wakefield generation, referring to the analogy with the wake driven by the bow of a boat moving through water, but the mechanism is similar (except it has the advantage that the plasma wave is driven linearly instead of as an instability).

In either case, the resulting electrostatic plasma wave can continuously accelerate relativistic electrons with enormous acceleration gradients [30]. The gradient can be estimated from Coulomb's law and the fact that because

$$\nabla \cdot \mathbf{E} \sim E\omega_p/c \propto E\sqrt{n_e},$$

then

$$E \sim \sqrt{n_e} \text{ eV/cm},$$

corresponding to 1 GeV/cm for $n_e = 10^{18}$ cm^{-3}. Because this gradient is four orders-of-magnitude greater than achieved by conventional accelerators (based on fields driven by radio-frequency waves pumped into metal cavities), laser-driven plasma accelerators have received considerable recent attention.

In the self-modulated regime, they have been shown to accelerate an amount of electron charge (100 nC) comparable to that from conventional accelerators and to have superior transverse geometrical emittance (product of divergence angle and spotsize, similar to the $f/\#$ in light optics). However, their longitudinal emittance is currently much inferior, energy spreads of 100%. They have been shown to be useful for much of the same applications: radio-isotope production, radiation chemistry, as well as X-ray, proton and neutron generation. Once the longitudinal emittance can be reduced, they may be advantageous for, among other applications, injectors (especially of short-lived unstable particles) into larger conventional accelerators for high-energy physics research and light sources, and, as discussed in Section 4, as stand-alone all-optically driven ultrashort-pulse duration X-ray sources. Dramatic reduction of the angular divergence of a laser accelerated electron beam was observed with increasing laser power above the relativistic self-focusing threshold [36], as shown in Fig. 4.

In the resonant regime, there have been some theoretical analysis and simulations done in the 80's and 90's [9,16]. In recent years, the Ti:sapphire laser using CPA technology can produce up to 50 TW of power with a pulse duration of 30 fs. With the availability of high power and short duration laser pulses, there have been many breakthroughs in experiments in the resonant regime [11,12,19,20,37]. Wang et al. first reported the experimental observation of an electron beam in this regime using an $f/\#3$ parabola [37]. Their electron energy was continuous due to the filamentation induced by the hot spot in the laser beam. Malka et al. showed that the electron energy from LWFA can reach to 200 MeV with a long focal length parabolic mirror, and the energy spread was 100% [19]. In their experiment, the laser pulse duration was about 4 times longer than the plasma period. But due to the group velocity difference in the front and back edge of the pulse (the front edge moves more slowly since more electrons were accumulated at the front), the laser pulse was self-compressed in the plasma and formed an optical shock. This resulted in an extremely sharp leading edge and was able to drive the relativistic plasma wave beyond its wave-breaking limit. In this case, there was no Raman scattering, but the laser spectrum became blue shifted and broadened. More recently, different research groups reported quasi-monoenergetic electron beams in this regime with 20% energy spread. The peak electron energy varies from 80 to 120 MeV. Mangles et al. from Rutherford and Geddes et al. from Berkeley National Lab explained this as the match of the interaction length with the dephasing length. In this condition, the electrons did not experience the deceleration so the energy did not spread [12,20]. However, Faure et al. from LOA argued that the monoenergetic electrons accelerated by the electric field formed behind the laser pulse and this theory was supported by a PIC simulation [11].

Most experiments on plasma wakefield acceleration are in the regime of $a_0^2 \sim 1$. The SIMLAC code has been used to study wakefield generation and laser propagation in the limit $a_0^2 \ll 1$ [29]. It draws from nonlinear optics models and treats propagation in the group velocity frame. In this idealized model (which assumes perfect Gaussian beams), the pulse and wake, are maintained over long enough propagation distance to accelerate an electron to GeV energy. A three-dimensional envelope equation for the laser field was derived that includes nonparaxial effects, wakefields, and relativistic nonlinearities [29].

8. Relativistic phase modulation

Analogous to self-focusing, which is due to the spatial refractive index modulation, the relativistic phase modulation of a high-intensity laser pulse is due to the refractive index modulation in the time domain. The time dependence of a laser usually can be described as a Gaussian distribution.

$$I = I_0 \exp\left(\frac{-T^2}{2T_0^2}\right), \tag{20}$$

where T_0 is the half-width (at $1/e$-intensity point), $T = t - z/v_g$ and v_g is the group velocity of the laser pulse in plasma.

As shown in Eq. (13), the time dependent laser intensity will result in a time dependent refractive index.

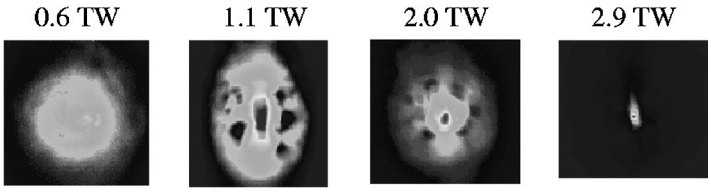

Fig. 4. Images of the spatial profiles of the electron beam measured by a CCD camera imaging a LANEX screen at a distance of 15 cm from the gas jet for various laser powers. The divergence angle of the beam decreases to a value of $\Delta\theta = 1^\circ$ at a power of 2.9 TW, corresponding to a transverse geometrical emittance of just $\epsilon_\perp \lesssim 0.06\pi$ mm mrad. Reproduced from [32].

The frequency shift is given by,

$$d\omega = -\frac{\omega}{c}\frac{\partial \eta}{\partial t}dx = -\frac{\omega}{c}n_2\frac{\partial I(t)}{\partial t}. \tag{21}$$

This equation shows that the frequency shift depends on the sign of $\partial I(t)/\partial t$. For the rising part of the laser pulse, $\partial I(t)/\partial t > 0$, and this causes the red-shifting of the laser pulse. Conversely, the falling edge of the laser pulse introduces a blue shift. A short pulse also has a finite frequency bandwidth and each component has different group velocity in the plasma, which causes the group velocity dispersion (GVD) effect and become severe when the laser pulse reaches tens of fs [6]. GVD effects also interplays with self-phase modulation and causes instabilities [28].

The frequency bandwidth of a transform limited Gaussian pulse can be estimated from Fourier analysis and is given by:

$$\tau = \frac{2(\ln 2)\lambda^2}{\pi \Delta\lambda c}, \tag{22}$$

where τ is the full width at half maximum (FWHM) of the laser pulse and c is the speed of light in vacuum. τ and T_0 are related by

$$\tau = 2(\ln 2)^{1/2}T_0 \approx 1.665T_0. \tag{23}$$

For instance, the bandwidth of a 400 fs laser pulse at 1.053 μm is at least 4.1 nm. Due to the mismatch between the stretcher and compressor, the duration of a laser pulse is usually larger than that of the transform-limited pulse.

Chen et al. report the observation of relativistic cross-phase modulation, which refers phase modulation of one light pulse by another copropagating pulse of different wavelength. In their particular case, a relativistically intense laser pulse phase-modulated a forward Raman scattering signal [4].

9. Interactions with solid-density targets

The generation of electrons by high-intensity laser light interacting with solid targets can generate energetic X-rays, accelerate other types of particles and induce nuclear reactions. For instance, high-order harmonics have been generated by the oscillation of the critical density surface, in the so-called moving mirror model [2]. Bright X-rays, originating from Bremstrahlung caused by electron collisions with high-Z atoms in solid-targets, have created isotopes by means of photofission. Laser-accelerated electron energies and angular distributions have been inferred from analyzing (γ, n) and $(\gamma, 2n)$ reactions in composite Pb/Cu targets and in Ta/Cu targets. Positrons were created by colliding laser-accelerated electrons with a tungsten target.

When electrons are heated to high temperatures or accelerated to high energies, they can separate from plasma ions. Such charge displacement creates an electrostatic sheath, which eventually accelerates the ions. The ions are pulled by the charge of the electrons and pushed by the other ions' unshielded charges (similar to the "Coulomb explosion" that can occur during the ionization of atoms). When the charge displacement is driven by thermal expansion, as in long-pulse (low power) laser-plasma experiments, the maximum ion energies are limited to less than 100 keV. However, when the charge displacement is driven by direct laser heating, as in short-pulse high-power laser-plasma experiments, multi-MeV ion energies are possible. This was first shown with gas jet targets, in which case the ions were accelerated radially into 2π, and then later with thin solid-density-films, in which case the ions were accelerated into collimated beams. In the latter case, hydrocarbons and water on the surface of the film can become ionized and provide a source of protons to be accelerated.

An intense laser can ponderomotively heat electrons. If the laser contrast is high, vacuum heating can occur in the following manner. When light encounters a sharp interface between vacuum and solid density, the electromagnetic field becomes evanescent in the region above the critical density. The instantaneous "$\mathbf{v} \times \mathbf{B}$" force can push electrons in the direction of the light's propagation vector; it also has a frequency twice that of the pump and a magnitude proportional to the square of the normalized vector potential, a_0^2. Thus, electrons can only complete half of their figure-eight orbits, on the vacuum side, gaining relativistic energies; they move through the overdense region without the electromagnetic field to pull them back. An electrostatic sheath can thus form, which will accelerate the ions left behind. Another important heating mechanism is stochastic heating, which occurs when the light that is reflected from the critical surface beats with the incoming wave to create a standing wave. The motion of electrons in such a wave can become chaotic, resulting in a large increase in electron temperature (> 100 keV).

As the heated electrons propagate through a solid, they can instantaneously field-ionize the neutral atoms of the solid. This will both modify the solid's conductivity and provide a source of protons on the rear-side of the target. If the film is thin enough, the electrons can pass through, and create a sheath on the rear-side of, the target. This latter mechanism has been dubbed the target normal sheath acceleration mechanism. The ions from thin foils have been claimed to originate from both the front and rear-side of the foil.

Several groups have reported the observation of ions originating from thin-film solid-density targets. Unlike previous long-pulse experiments, the ions were accelerated along the direction normal to the side of the target that is opposite to that upon which the laser was incident. The ions generally originate from water or hydrocarbons on the surface of the material. The acceleration results from several different mechanisms, which may be occurring simultaneously. Charge-displacement is again common to all, with the electrons being heated ponderomotively, such as by Brunel [3], $J \times \mathbf{B}$ or stochastic heating. In one case, the electrostatic sheath is formed at the backside of the ionization layer formed on the side of the target upon which the laser is incident (front side). In another case, the electrostatic sheath is formed by field ionization of the ion layer on the opposite side of the thin film target (back-side), the target normal sheath acceleration (TNSA) hypothesis. Numerical simulations show evidence for both front and back-side acceleration.

The results of these experiments indicate that a large number of protons ($10^{13} p$) can be accelerated, corresponding to source current densities (10^8 A/cm^2) that are nine orders-of-magnitude higher than produced by cyclotrons, but with comparable, or even lower, transverse emittances ($\epsilon_\perp \leqslant 1.0\pi$ mm mrad). Proton energies up to 60 MeV have been observed in experiments at intensities exceeding 10^{20} W/cm^2 (using a petawatt power laser). The high end of the proton spectrum typically has a sharp cut-off, but is a continuum. In one experiment, protons were observed to be emitted in ring patterns, the radii of which depend on the proton energy, which was explained by self-generated magnetic fields.

The production of radionuclides have been used as an ion energy diagnostic. In another example of a nuclear reaction initiated by an intense laser, neutrons have been produced by the He fusion reaction in the focus of 200 mJ, 160 fs Ti:sapphire laser pulses on a deuterated polyethylene target. Optimizing the fast electron and ion generation by applying a well-defined prepulse led to an average rate of 140 neutrons per shot. Neutrons have also been generated from cluster plasmas [7], which were produced by the cooled-nozzle, but with significantly lower laser intensities than required with planar solid targets.

10. Concluding remark

Clearly, this new field of relativistic nonlinear optics would not exist today without Einstein's contributions to our understanding of the physical principles that underlie it. This is just one of many examples (several of which were discussed in this special issue) that illustrate how the impact of Einstein's miracle year is still being felt a century later. Others will surely follow as the power of lasers continues to increase in the future, with no foreseeable limit.

Acknowledgements

The authors wish to thank the support of the National Science Foundation and the Chemical Sciences,

Geosciences and Biosciences Division of the Office of Basic Energy Sciences, Office of Science, US Department of Energy, as well as S.Y. Chen, S. Sepke, S. Banerjee, F. He, and Y.Y. Lau for their helpful comments.

References

[1] S. Banerjee, A. Maksimchuk, R. Shah, S. Sepke, A. Valenzuela, D. Umstadter, Phys. Rev. Lett. 95 (2005) 035004.
[2] B. Bezzerides, R. Jones, D. Forslund, Phys. Rev. Lett. 49 (1982) 202.
[3] F. Brunel, Phys. Rev. Lett. 59 (1987) 52.
[4] S. Chen, P. Zhang, N. Saleh, M. Rever, A. Maksimchuk, W. Theobald, D. Umstadter, Observation of relativistic cross-phase modulation in high intensity laser-plasma interactions, Phys. Rev. Lett. (2005), submitted for publication.
[5] S.-Y. Chen, A. Maksimchuk, D. Umstadter, Nature 396 (1998) 653.
[6] C.D. Decker, W.B. Mori, Phys. Rev. E 51 (1995) 1364.
[7] T. Ditmire, Opt. Photon. News 13 (2002) 28.
[8] J.H. Eberly, J. Opt. Soc. Am. B 3 (1986) 1324.
[9] E. Esarey, P. Sprangle, J. Krall, A. Ting, IEEE Trans. Plasma Sci. 24 (1996) 252.
[10] E. Esarey, P. Sprangle, J. Krall, A. Ting, IEEE J. Quantum Electron. 33 (1997) 1879.
[11] J. Faure, Y. Glinec, A. Pukhov, S. Kiselev, S. Gordienko, E. Lefebvre, J.-P. Rousseau, F. Burgy, V. Malka, Nature 431 (2004) 541.
[12] C.G. Geddes, C. Toth, J. van Tilborg, E. Esarey, C.B. Schroeder, D. Bruhwiler, C. Nieter, J. Cary, W.P. Leemans, Nature 431 (2004) 538.
[13] P. Gibbon, E. Förster, Plasma Phys. Controlled Fusion 38 (1996) 769.
[14] F. Hartemann, High-Field Electrodynamics, CRC Press, Boca Raton, 2001.
[15] C.J. Joshi, P.B. Corkum, Phys. Today 48 (1995) 36.
[16] T. Katsouleas, Phys. Rev. A 33 (1986) 2056.
[17] Y.Y. Lau, F. He, D. Umstadter, Phys. Plasmas 10 (2003) 2155.
[18] B. Luther-Davies, E.G. Gamaly, Y. Wang, A.V. Rode, V.T. Tikhonchuk, Sov. J. Quantum Electron. 22 (1992) 289.
[19] V. Malka, S. Fritzler, E. Lefebvre, M.-M. Aleonard, F. Burgy, J.-P. Chambaret, J.-F. Chemin, K. Krushelnick, G. Malka, S.P.D. Mangles, Z. Najmudin, M. Pittman, J.-P. Rousseau, J.-N. Scheurer, B. Walton, A.E. Dangor, Science 298 (2002) 1596.
[20] S.P.D. Mangles, C.D. Murphy, Z. Najmudin, A.G.R. Thomas, J.L. Collier, A.E. Dangor, E.J. Divall, P.S. Foster, J.G. Gallacher, C.J. Hooker, D.A. Jaroszynski, A.J. Langley, W.B. Mori, P.A. Norreys, F.S. Tsung, R. Viskup, B.R. Walton, K. Krushelnick, Nature 431 (2004) 535.
[21] C. Max, J. Arons, A.B. Langdon, Phys. Rev. Lett. 33 (1974) 209.
[22] A. Maksimchuk, et al., Plasma Phys. Rep. 30 (2004) 473.
[23] J. Meyer-ter-Vehn, A. Pukhov, Z.-M. Sheng, Relativistic laser plasma interaction, in: D. Batani (Ed.), in: Atoms, Solids and Plasmas in Super-Intense Laser Fields, Kluwer Academic, Plenum, New York, 2001, p. 167.
[24] G. Mourou, D. Umstadter, Phys. Fluids B 4 (1992) 2315.
[25] G. Mourou, D. Umstadter, Sci. Am. 81 (2002).
[26] G. Mourou, C.P.J. Barty, M.D. Perry, Phys. Today 56 (1998) 22.
[27] B. Quesnel, P. Mora, Phys. Rev. E 58 (1998) 3719.
[28] P. Sprangle, B. Hafizi, J.R. Peñano, Phys. Rev. E 61 (2000) 4381.
[29] P. Sprangle, J.R. Peñano, B. Hafizi, R.F. Hubbard, A. Ting, D.F. Gordon, A. Zigler, T.M. Antonsen Jr., Phys. Plasmas 9 (2002) 2364.
[30] T. Tajima, J.M. Dawson, Phys. Rev. Lett. 43 (1979) 267.
[31] T. Tajima, G. Mourou, Phys. Rev. ST Accel. Beams 5 (2002) 031301.
[32] D. Umstadter, Phys. Plasmas 8 (2001) 1774.
[33] D. Umstadter, J. Phys. D: Appl. Phys. 36 (2003) R151.
[34] D. Umstadter, T.B. Norris (Eds.), IEEE J. Quantum Electron. 33 (1997) 1877.
[35] D. Umstadter, Relativistic nonlinear optics, in: B.D. Guenther, D.G. Steel, L. Bayvel (Eds.), Encyclopedia of Modern Optics, Elsevier, Oxford, 2004, p. 289.
[36] R. Wagner, S.-Y. Chen, A. Maksimchuk, D. Umstadter, Phys. Rev. Lett. 78 (1997) 3125.
[37] X. Wang, M. Krishnan, N. Saleh, H. Wang, D. Umstadter, Phys. Rev. Lett. 84 (2000) 5324.